J. Membrane Biol. 187, 203–211 (2002)
DOI: 10.1007/s00232-001-0164-4

The Journal of
Membrane
Biology

Secretion Pores in Human Endothelial Cells during Acute Hypoxia

T. Goerge, A. Niemeyer, P. Rogge, R. Ossig, H. Oberleithner, S.W. Schneider
Department of Physiology, University of Münster, Robert-Koch-str. 27a, D-48149 Münster, Germany

Received: 1 November 2001/Revised: 28 February 2002

Abstract. Weibel-Palade bodies (WPB) are endothelial vesicles that store von Willebrand factor (vWF), involved in the early phase of hemostasis. In the present study we investigated the morphodynamics of single WPB plasma membrane fusion events upon hypoxic stimulation by using atomic force microscopy (AFM). Simultaneously, we measured vWF release from endothelial cells to functionally confirm WPB exocytosis.

Exposing human endothelial cells to hypoxia (pO_2 = 5 mm Hg) we found an acute (within minutes) release of vWF. Despite acute vWF release, potential cellular modulators of secretion, such as intracellular pH and cell volume, remained unchanged. We only detected a slight instantaneous increase of cytosolic Ca^{2+} concentration. Although overall cell morphology remained virtually unchanged, high resolution AFM images of hypoxic endothelial cells disclosed secretion pores, most likely the loci of WPB exocytosis on luminal plasma membrane.

We conclude that short-term hypoxia barely alters overall cell morphology and intracellular milieu. However, at nanometer scale, hypoxia instantaneously switches the smooth luminal plasma membrane to a rough activated cell surface, covered with secretion pores that release vWF to the luminal cell surface.

Key words: vWF — Exocytosis — Cell volume — HUVEC — AFM — Intracellular calcium

Introduction

The vascular endothelium with its salient location at the interface between blood and tissue plays a pivotal role in the process of regulation of blood pressure, blood coagulation and inflammation. The transition into a procoagulatory and proinflammatory state upon stimulation is referred to as endothelial cell (EC) activation [7]. One fundamental characteristic of this activation is the induction of exocytosis [29]. Exocytosis is defined as vesicle transport to the plasma membrane with subsequent membrane fusion and release of vesicle content into the extracellular space [13]. During this process, Weibel-Palade bodies, intracellular 2×0.1-μm^2 large rodlike shaped vesicles, fuse with the plasma membrane. WPBs play a dual role in EC activation, promoting both a procoagulatory and a proinflammatory answer [25, 29, 43]. WPBs are storage sites of vWF, a glycoprotein involved in hemostasis as a mediator of platelet adhesion to the endothelium and of platelet-platelet aggregation [32]. In addition to vWF release, P-selectin (CD62P), an adhesion protein necessary for leukocyte binding to sites of inflammation, is translocated to the plasma membrane [27].

Exocytosis of WPBs has been shown to be inducible by different secretagogues that cause exocytosis in a specific pattern [5, 14, 42]. These agonists (most of them mediators of thrombosis and inflammation) can be classified by their appropriate intracellular mediator into Ca^{2+}-raising and cAMP-raising agonists. Most agonists induce WPB exocytosis by a Ca^{2+}-mediated pathway [9, 14, 16, 24, 41]. Despite the high pathophysiological relevance, the cellular mechanisms involved in the acute phase of regulated hypoxia-induced exocytosis remain poorly understood [27, 41].

Cellular responses to hypoxia can be acute or chronic [22]. In the present paper, we investigated the morphologic alterations of the endothelial cell surface in the acute phase of hypoxic stimulation. By AFM, alterations in cell surface topography can be identified [34, 36]. In addition, we measured intracellular Ca^{2+} concentration to assess its involvement as intracellular mediator at the onset of hypoxic stimulation.

Concomitantly, we measured the vWF level in the cell supernatant to quantify hypoxia-induced

Correspondence to: S.W. Schneider; email: sschnei@uni-muenster.de

WPB exocytosis. The combination of these techniques allows the exploration of an intracellular process and the subsequent visualization of its effect on the plasma membrane. In this study we concentrate on the acute phase of hypoxia, observing the first pathophysiological cell alterations.

Materials and Methods

Endothelial Cells and Cell Culture

Human umbilical vein endothelial cells (HUVEC) were isolated and grown in culture as described [15]. For experiments we used confluent endothelial cells not older than 10 days (passage 1). The culture medium (Gibco, Karlsruhe, Germany) contained 10% heat-inactivated fetal calf serum (Boehringer Mannheim, Mannheim, Germany), antibiotics (penicillin, streptomycin), 5U/ml heparine (Biochrom, Berlin, Germany), and 1 ml/100 ml growth supplement derived from bovine retina as described [19].

Exposure to Hypoxia and vWF Determination

HUVEC were cultured either on gelatine-coated glass coverslips (diameter = 2 cm) in petri dishes or in 12-well gelatin-coated tissue culture plates (Falcon, New Jersey). HUVEC reached confluence within 5 days. The cells were exposed to normoxia or hypoxia in an incubation chamber at 37°C, 100% humidity with pO_2 at 160 or 5 ± 0.3 mmHg, respectively. pO_2-concentrations were constantly monitored with an O_2-optode (MOPS-1, Comte-Analysesysteme, Hannover, Germany). This instrument is based on an oxygen-sensitive dye (Tris(4,7-diphenyl-1,10-phenanthrolin)-ruthenium (II)-chloride) immobilized on one end of an optical fiber [11].

The dye is excited at 470 nm wavelength and the hypoxia-dependent fluorescent response is continuously measured. Cells were incubated in (mmol/l): 140 NaCl; 5 KCl; 1 $MgCl_2$; 1 $CaCl_2$; 5 glucose; 10 HEPES(N-2-hydroxyethylpiperazine-N′-2-ethanesulfonic acid) further referred to as HEPES-buffered Ringer solution (HBRS). Hypoxic and normoxic HBRS were both prepared by equilibration with 100% N_2 and room air, respectively, for 10 minutes in the incubator chamber. Solutions have been treated equally in terms of bubbling. The change of volume was less than 1% after 60 minutes of incubation. Hypoxic HBRS added to the cells had a pO_2 of 5 mmHg. As monitored by the O_2-optode this level did not change during the whole experiments, as long as the incubation chamber was perfused with N_2. Endothelial cells from the same umbilical cord were used each time for the hypoxic and control group in order to avoid scatter due to heterogeneity of ECs, as recently discussed [21]. The supernatant of endothelial cells exposed to hypoxia or normoxia was harvested, cleared of cell debris by centrifugation and immediately stored at –20°C for later vWF analysis. The release of vWF was measured by a sandwich ELISA technique [19], using a polyclonal rabbit anti-human vWF antibody (DAKO, Hamburg, Germany) and a polyclonal rabbit peroxidase-labeled anti-human vWF antibody. The standard curve was generated using standard human plasma (SHP) (Behring, Marburg, Germany). Results are indicated as the percentage of the vWF concentration of SHP. 100% SHP is equivalent to about 10 μg/ml.

Cell Viability

In order to exclude cell deterioration as a cause for elevated vWF levels, we tested post-experimental cell viability by two different means. Morphological aspects were documented by the trypan blue exclusion method. Less than 5% of the cell membranes were found damaged even after 60 minutes of hypoxia, thus not exceeding the percentage found in the normoxic group. In addition, post-experimental vWF release as a functional means of viability was measured upon 50 μM histamine (Sigma, Steinheim, Germany) stimulation. Histamine-induced vWF secretion is provocable even after one hour of hypoxia.

Surface Scanning and Cell Volume Measurements with Atomic Force Microscopy

To further investigate hypoxia-induced alterations in endothelial cell surface morphology, we incubated cells after removal of the supernatant in 3% isoosmolar glutaraldehyde. After 10 minutes of fixation, cells were intensively rinsed in isoosmolar HBRS and imaged in HBRS with atomic force microscopy (AFM). AFM is based on the deflection of a fine silicon nitride tip scanning the surface of a sample [4]. AFM reconstructs an image of a surface from x, y and z data to develop a three-dimensional topography of any surface at a nanometer level. The procedure for AFM imaging in contact and tapping mode of different biological samples was described elsewhere [31]. In previous experiments we used AFM to study exocytotic events in the apical surface of pancreatic epithelial cells. In these experiments we visualized exocytotic pores after cell stimulation [36]. In addition to imaging and analyzing surface topography, AFM enables one to measure cell volume of individual adherent cells [35] with a femtoliter resolution and isolated proteins, such as vWF [38], in a physiological environment. Volume measurements on epithelial and endothelial cells were already described [30, 35]. For our experiments we used the BioScope^{RM} (Digital Instruments, Santa Barbara, CA) in conjunction with an inverted optical microscope (Zeis Axiovert). Silicon-nitride tips were used in contact and tapping mode (resonance frequency between 7 to 9 kHz) with a spring constant of 8 mNm^{-1} (Park Scientific, Sunnyvale, CA). We applied a vertical force of about 0.4–1.0 nN during contact mode. AFM images were generated at line frequencies of 1 to 2 Hz, with 512 lines per image. After cell imaging the 3-dimensional data (cell volume, cell morphology) was analyzed by the software coming with the instrument (Digital Instruments).

Measurements of Intracellular Calcium

Endothelial cells were cultured on glass coverslips coated with 0.5% gelatine. After the cells were grown to confluency they were loaded with 1 μM fura2/AM in HBRS for 10 min at room temperature. Then the coverslips were mounted on a temperature-controlled (37°C) microscope tissue chamber and washed three times with HBRS before the onset of continuous superfusion. Fields of about 8 cells were visualized on a Nikon (Diaphot 300) inverted microscope and excited alternately at 340 nm and 380 nm. The fluorescence emission was measured at 510 nm using a photon counting detector. The 340 nm and 380 nm tracings were corrected in each experiment for autofluorescence before calculating the 340/380 ratio. Calculation of the intracellular Ca^{2+} concentrations $[Ca^{2+}]_{in}$ was performed as described by Grynkiewicz et al. [12]. During one experiment we averaged the calcium concentration out of ~8 endothelial cells. Hypoxia was applied by superfusing the cells with preconditioned hypoxic solution in a hypoxic atmosphere. All experiments were performed under tight control of constant pH, temperature, vaporization saturation and pO_2 (measured by the above mentioned pO_2-optode).

Measurements of Intracellular pH

Intracellular pH ($[pH]_{in}$) measurements were performed like measurements of $[Ca^{2+}]_{in}$ except for the following deviations: We used

the fluorescent dye BCECF-AM and excited at 440 and 480 nm wavelength. Calibration was performed at different pH values (pH values: 6.4, 6.8, 7.2, 7.6) using high-potassium, low-sodium HBRS (mimicking intracellular conditions), that contained nigericine (10 μmol/l). In an individual experiment we averaged the $[pH]_{in}$ obtained from ~8 endothelial cells.

Statistcal Analysis

Mean data of experiments are given ± standard error of the mean (SE). Statistical significance was tested with unpaired Student's *t*-test. * indicates a significant difference of compared values ($P \leq 0.05$).

Results

Acute vWF Secretion upon Hypoxic Stimulation

To explore whether hypoxic conditions acutely (5–10 minutes) activate HUVECs to generate a procoagulatory and proinflammatory milieu, we determined the vWF release, as an indicator of WPB exocytosis, in hypoxia-stimulated and normoxic cells. Figure 1*A* summarizes the results obtained from approximately 30 umbilical cords. Half of the isolated cells from the same umbilical cord were used as the normoxic control group. Since basal vWF release exhibits a rather large scatter due to the heterogeneity of different umbilical cords, results are expressed as a relative increase to the corresponding normoxic group from the same umbilical cord. Upon hypoxic stimulation, we found an acute increase of vWF concentration in the cell supernatant. After 5 minutes of incubation the vWF concentration was 1.8-fold higher compared with the normoxic group (normoxia: 32 ± 3.5 μg/l; hypoxia: 60 ± 8.4 μg/l, both $n = 13$). The data show that the hypoxia-induced vWF release is an acute event with the major release taking place during the first 5 minutes. A prolonged (more than 5 minutes) hypoxic stimulation did not further increase vWF release.

Co-Stimulation with Histamine Increases the Hypoxic Response

In order to evaluate the extent of hypoxia-induced vWF release, we used the common secretagogue as a stimulus of reference. Endothelial cells exposed to both hypoxia and histamine (50 μmol/l) were compared to hypoxia-stimulated cells in absence of histamine. The stimulation of endothelial cells with histamine under hypoxic conditions showed a 3.5-fold elevated release of vWF compared to hypoxia alone (Fig. 1*B*). This indicates that hypoxia is a potent, though rather weak stimulus compared to histamine. Therefore, we conclude that hypoxic stimulation recruits only a small fraction of WPBs, whereas histamine (within 5 minutes of incubation) recruits almost

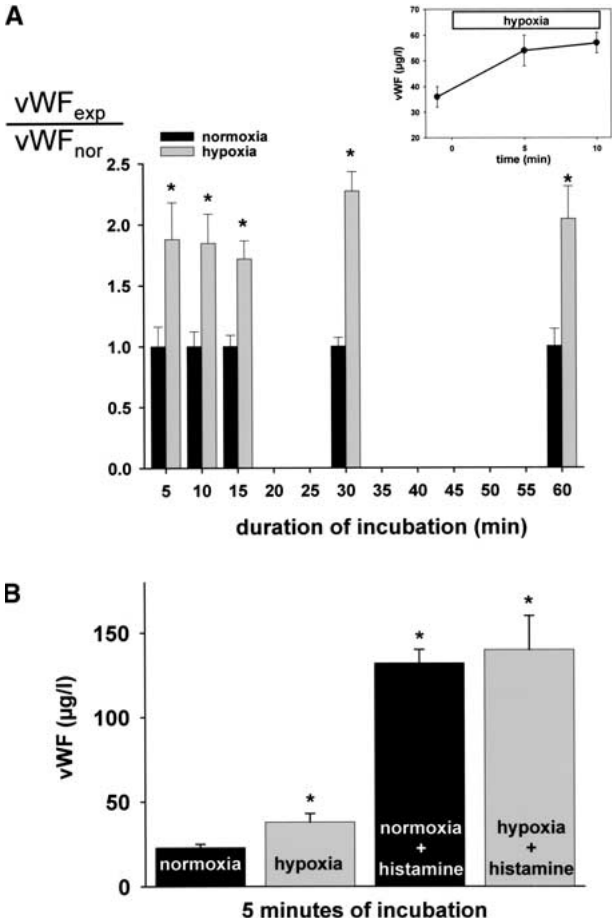

Fig. 1. Cumulative release of vWF during normoxic and hypoxic (pO_2 = 5 mm Hg) conditions. (*A*) The paired columns represent individual experiments. Number of experiments varies between 11 and 26. vWF_{exp} = vWF release during hypoxic stimulation (grey) or during normoxic conditions (black). vWF_{nor} = vWF release during normoxic incubation. Asterisks indicate significant differences between normoxic and hypoxic mean values. Please note that the values indicate cumulative release of vWF, which represents the total amount of secreted vWF over the indicated time periods. The inset represents a paired experiment switching from normoxic to hypoxic conditions. (*B*) Effect of hypoxia and histamine stimulation. HUVEC were incubated in a histamine-containing hypoxic solution (right column). Hypoxia-induced vWF exocytosis was 38 ± 5 μg/l ($n = 5$), whereas histamine-induced vWF exocytosis under hypoxic conditions was 139 ± 20 μg/l ($n = 5$). The normoxic cell released a vWF concentration of 23 ± 2 μg/l ($n = 5$) into the supernatant. Histamine-induced vWF exocytosis under normoxic conditions was 125 ± 10 μg/l ($n = 5$). Asterisks indicate significant differences between stimulated and normoxic mean values. Mean values of histamine stimulation do not differ significantly during normoxic and hypoxic stimulation.

all WPBs to undergo exocytosis, independent of hypoxic or normoxic incubation. After 5 minutes of histamine stimulation, subsequent immunofluorescent staining of vWF reveals an almost complete depletion of WPB within HUVEC (*data not shown*).

In addition, the common secretagogue histamine was used as a further method to test viability of

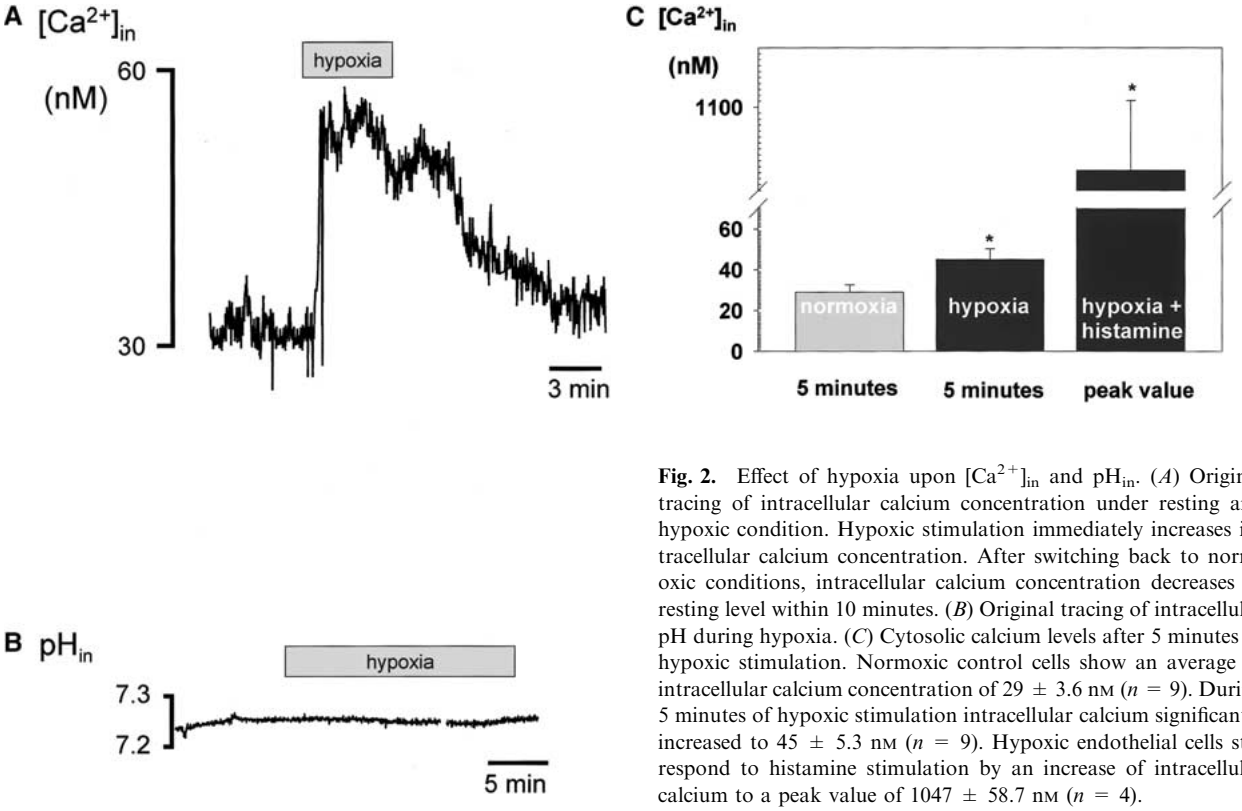

Fig. 2. Effect of hypoxia upon $[Ca^{2+}]_{in}$ and pH_{in}. (*A*) Original tracing of intracellular calcium concentration under resting and hypoxic condition. Hypoxic stimulation immediately increases intracellular calcium concentration. After switching back to normoxic conditions, intracellular calcium concentration decreases to resting level within 10 minutes. (*B*) Original tracing of intracellular pH during hypoxia. (*C*) Cytosolic calcium levels after 5 minutes of hypoxic stimulation. Normoxic control cells show an average of intracellular calcium concentration of 29 ± 3.6 nM (n = 9). During 5 minutes of hypoxic stimulation intracellular calcium significantly increased to 45 ± 5.3 nM (n = 9). Hypoxic endothelial cells still respond to histamine stimulation by an increase of intracellular calcium to a peak value of 1047 ± 58.7 nM (n = 4).

endothelial cells under hypoxic conditions. After stimulation with histamine, hypoxia-incubated HUVEC responded with a further increase of vWF exocytosis. After 60 minutes of hypoxic stimulation the same cells were stimulated with histamine. After histamine stimulation HUVEC respond with a further increase (2.5-fold; n = 5) of vWF release.

Immediate Hypoxia-induced Increase of Intracellular Calcium at Unaltered Intracellular pH

An increase of intracellular calcium has been demonstrated to be the mediator of regulated exocytosis [14, 24, 34]. Therefore, we measured the intracellular calcium concentration under normoxic and hypoxic conditions. The original tracing (Fig. 2*A*) demonstrates a representative experiment. A plateau value is reached within 2 minutes and remains stable during hypoxia. After going back to normoxic conditions the calcium level slowly recovers to resting level. In a second set of experiments we measured the intracellular pH (pH_{in} = 7.2 ± 0.03; n = 8) during hypoxic stimulation. We did not find any intracellular pH alterations during 40 minutes of hypoxic incubation (n = 5) (Fig. 2*B* original tracing). In an additional series of experiments we measured intracellular calcium upon hypoxic and histamine stimulation. After switching to hypoxic conditions we saw an immediate intracellular calcium increase to a new steady state of ~50 nM. After stimulation with histamine we measured a calcium increase to a peak value of about 1 μM. Figure 2*C* summarizes the experiments. During resting conditions we measured an intracellular calcium concentration of 29 ± 1.3 nmol/l (n = 9). After switching to hypoxia, intracellular calcium concentration immediately increased to a new steady state of 45 ± 5.3 nmol/l (n = 9) (Fig. 2*C*). Following stimulation with histamine the cytosolic calcium concentration increased to a peak value of 1047 ± 58.7 nmol/l (n = 4). The calcium spike after histamine stimulation is known to be due to an intracellular IP_3-dependent calcium release [24]. The histamine-induced calcium increase was similar in normoxic and hypoxic ECs.

Extracellular Calcium Is a Prerequisite for Acute vWF Exocytosis

In order to investigate whether extracellular calcium accounts for the acute increase of intracellular calcium and vWF release, we measured the amount of hypoxia-induced exocytosis of vWF in calcium-free EGTA-buffered (3 mmol/l) HBRS. Figure 3 summarizes the results of 20 experiments. Ca^{2+}-free HBRS inhibits the hypoxia-induced vWF secretion. The constitutive vWF release in normoxic cells is not affected by the omission of calcium from HBRS.

In conclusion, the histamine-induced intracellular calcium increase was unaffected during hypoxic

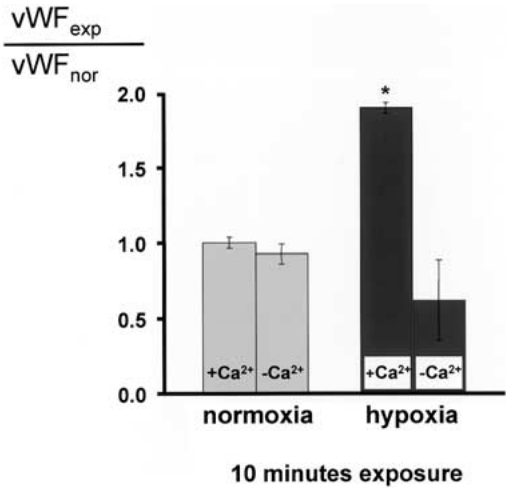

Fig. 3. vWF secretion after 10 minutes of incubation in Ca^{2+}-free medium. The normoxic release in HBRS is set as one, the experimental results expressed as ratios derived from ELISA. vWF_{exp} = vWF release upon hypoxic stimulation or during Ca^{2+}-free incubation. vWF_{nor} = vWF release during normoxic control conditions. Exocytosis of vWF induced upon hypoxic stimulation is significantly blocked in Ca^{2+}-free medium. Number of experiments = 4 for each column.

conditions indicating intact calcium stores during hypoxia. Moreover, vWF release upon hypoxic stimulation was abolished in a calcium-free buffer solution. Therefore, it is very likely that the hypoxia-induced calcium increase is due to plasma membrane calcium influx followed by vWF secretion.

Acute Hypoxia Does not Increase Endothelial Cell Volume

To investigate alterations in cell volume following hypoxia, we measured cell surface topography of endothelial cells by using AFM. AFM enables one to perform measurements of cell volume in adherent cells. Cell volume and cell topography can be obtained simultaneously on a single cell. Imaging was performed in HBRS. An area of 100×100 μm^2 was imaged that contained about 7 cells (Fig. 4*A*). The normoxic group revealed an average cell volume of 2980 ± 74 fl ($n = 26$) compared to the hypoxic group with an average cell volume of 2868 ± 121 fl ($n = 23$) (Fig. 4*B*). The data show that cell volume of HUVEC exposed to 5 minutes of hypoxic stimulation is not different from the cell volume of normoxic cells. An unaffected cell volume and a constant intracellular pH (*see* above) support the hypothesis of stable energy conditions in hypoxic ECs.

Secretion Pore Formation during Acute Hypoxia

Besides a micrometer resolution for whole-cell imaging, AFM enables one to measure surface

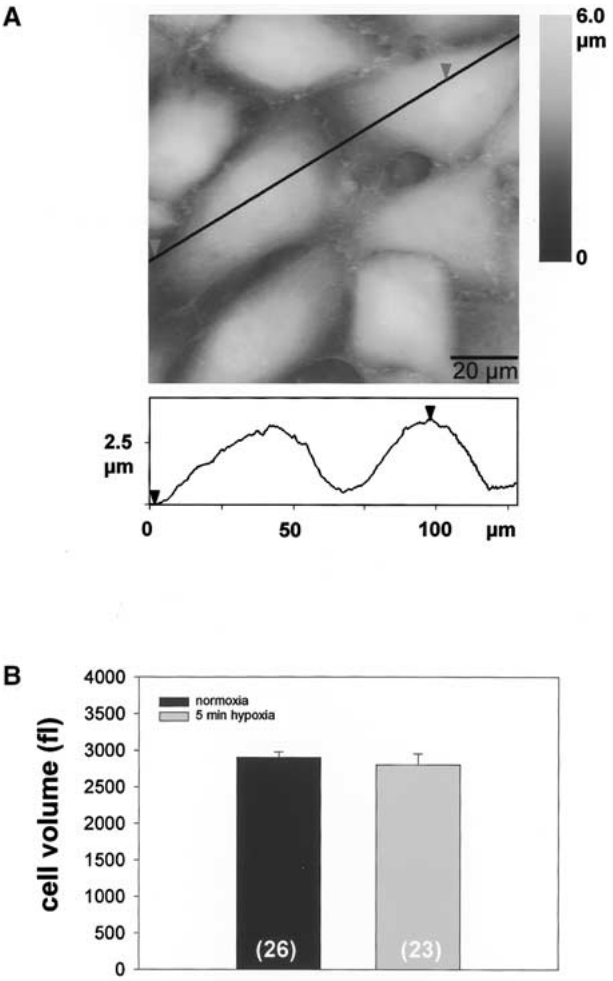

Fig. 4. Low magnification of HUVEC surface topography. (*A*) 3-dimensional image of 7 endothelial cells 5 minutes after hypoxic stimulation. The height of the cells is indicated by brightness (*see* bar). A 2-dimensional section of two endothelial cells was made to show the cell height. The cell height between the two arrows, one arrow on glass, the second on the cell, is 3.4 µm. (*B*) Cell volume of HUVEC after 5 minutes of hypoxic incubation. Cell volume of hypoxic cells was virtually unchanged compared to normoxic cell.

topography in more detail. To gain high resolution we imaged small cell surface areas ($\sim 10 \times 10$ μm^2). Figure 5*A* shows representative images of a normoxic and a hypoxic cell. Normoxic cells show a large number of humps ($1.7 \pm 0.26/10$ μm^2; diameter: 1–2 µm; height above plasma membrane level: 150–250 nm, $n = 18$). After hypoxic stimulation the number of humps decreased, whereas vWF secretion increased. We found pore-like structures (diameter: 300–800 nm) in the plasma membrane of hypoxic cells. These pore–like structures were also found after histamine stimulation. The decrease of humps and the increase of exocytotic pores correlate qualitatively with the amount of vWF release (Fig. 5*B*). Histamine-stimulated cells exhibit about 0.9 ± 0.08

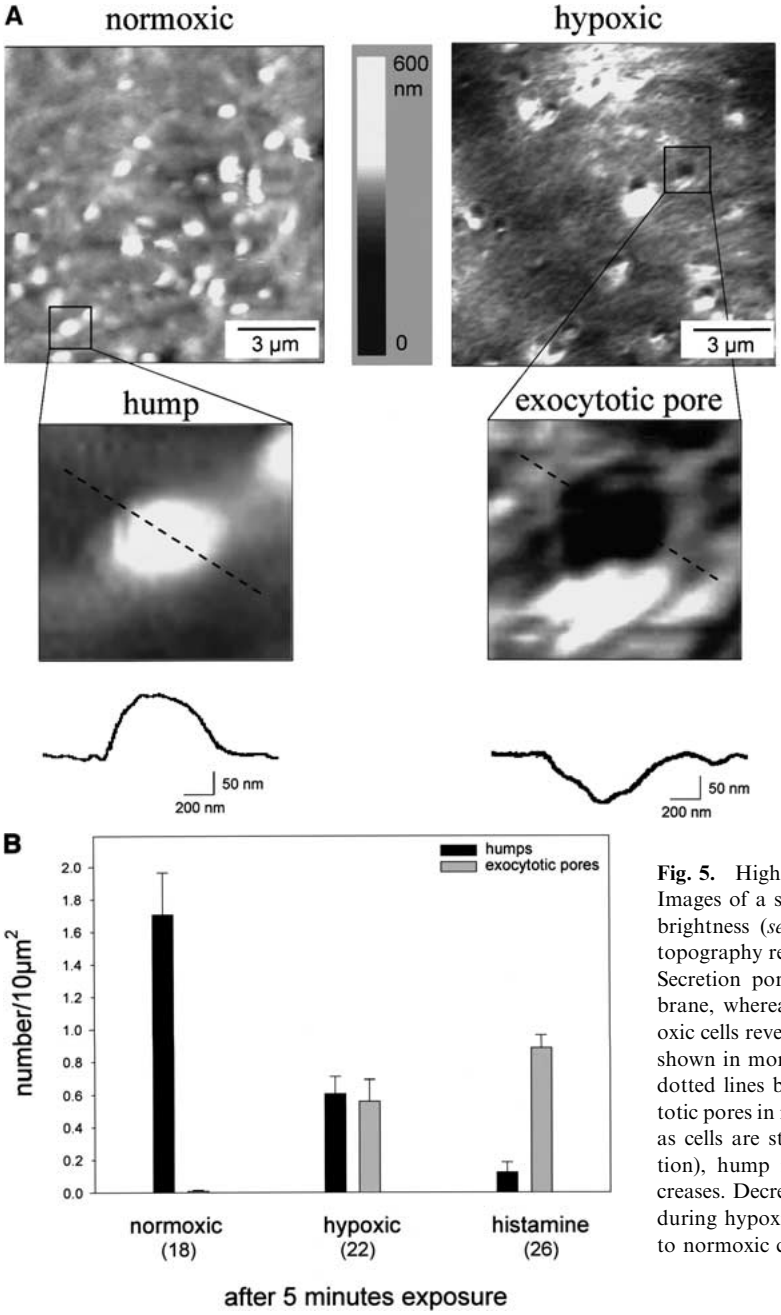

Fig. 5. High magnification of HUVEC surface topography. (*A*) Images of a small cell surface area are shown. Height is given by brightness (*see* bar). After hypoxic stimulation (5 min), surface topography reveals secretion-pore formation in addition to humps. Secretion pores indicate WPB fusion events with plasma membrane, whereas humps represent subplasmalemmal WPB. Normoxic cells reveal only humps and no pores. A hump and a pore are shown in more detail with the respective height profiles along the dotted lines below the images. (*B*) Number of humps and exocytotic pores in normoxic, hypoxic or histamine-treated cells. As soon as cells are stimulated (hypoxic incubation or histamine stimulation), hump number decreases and exocytotic pore number increases. Decrease of humps, as well as increase of secretion pores, during hypoxia or histamine stimulation are significant compared to normoxic cells.

pores/10 μm^2 (n = 22) and 0.1 ± 0.06 humps/10 μm^2 (n = 22), whereas in hypoxic-stimulated cells (less vWF release compared to a histamine-induced vWF release) we found 0.6 ± 0.13 pores/10 μm^2 (n = 26) and 0.6 ± 0.10 humps/10 μm^2 (n = 26). Pores were virtually absent in normoxic or unstimulated cells. To confirm that pores are release sites of vWF, we did immunofluorescence stainings of vWF on the same sample (first antibody: rabbit anti-human vWF, antibody; second antibody: FITC-labeled anti-rabbit). Using laser scanning microscopy we found vWF spots on the luminal membrane located where pores were identified. Furthermore, the geometry of humps and pores matches the size of WPBs. To our knowledge no secretory vesicles sensitive to histamine stimulation and with a comparable geometry exist in ECs [24]. Therefore, the data strongly suggests that the pores appear as the result of WPB fusion during exocytosis with the plasma membrane and, therefore, most likely represent secretion pores. The humps are subplasmalemmal WPB that are ready to fuse with the plasma membrane if stimulation occurs.

Discussion

The present study shows that hypoxia activates ECs within seconds (intracellular calcium) to minutes (vWF exocytosis). This rapid activation is consistent with the clinical observation that ischemic events result in an acute elevated vascular procoagulatory and inflammatory response [26, 37]. The pathophysiological need for increased vWF levels during hypoxia is understood as a mechanism initiating tissue repair and remodeling at the ischemic site [27, 37].

Previous studies on human umbilical venous endothelial cells have shown that the procoagulatory and inflammatory response evoked by chronic ischemia is characterized by secretion of von Willebrand factor and P-selectin with a statistically significant increase after 2 hours [27]. The slower EC activation shown by other authors may be due to the different experimental setups to study hypoxic effects on ECs. Preliminary experiments revealed that a meticulous control of temperature, pH, atmospheric humidity and pO_2 is indispensable, as endothelial cells are very sensitive to changes in the surrounding milieu. Moreover, the delicacy of establishing a defined hypoxic milieu is a matter of recent discussion [1]. Taking these findings into account, we constructed an incubation chamber that guarantees a permanent monitoring of the above stated parameters. A newly designed pO_2 optode continuously measured the oxygen concentration and all experiments were performed at 5 mmHg $\pm$ 0.3 mmHg pO_2 [11]. Since application of a hypoxic atmosphere is insufficient to achieve hypoxic conditions in the cell supernatant, all buffers were equilibrated with nitrogen. Thus, our approach distinctly differs from previous studies, in which hypoxia-induced vWF secretion was expected to occur by placing the cells in a hypoxic atmosphere. As oxygen diffusion from the medium into the atmosphere is a rather slow process, it might account for the latency of the cellular response in previous studies. In our approach, however, hypoxic conditions are instantly achieved at the cellular level and, therefore, acute effects of isolated hypoxia can be observed. Future studies with application of 2-deoxy-D-glucose and concomitant acidosis will reveal the onset of ischemic endothelial cell activation. This present approach demonstrated for the first time that HUVEC respond to isolated hypoxic stimulation with an acute release of von Willebrand factor by WPB exocytosis. 5 minutes of hypoxia are sufficient to significantly raise the amount of secreted von Willebrand factor.

Endothelial cell activation, in particular exocytosis, can also be confirmed by morphological alterations. However, since vesicle fusion with the plasma membrane is thought to cause morphological alterations at the nanometer scale, a high-resolution instrument for imaging plasma membrane topography is necessary. AFM fulfills the prerequisites for imaging and analyzing such fusion events [20, 36]. The presented data strongly suggest that a pool of WPBs in normoxic unstimulated endothelial cells is localized underneath the plasma membrane appearing as humps. These vesicles are able to fuse instantaneously with the plasma membrane upon hypoxic stimulation. Fusion events are visible as pore-like structures. This pore formation most likely represents WPB exocytosis. The decrease in the number of humps on EC surface is an excellent qualitative indicator for vWF release. Numerous in unstimulated cells, the number of humps significantly decreases upon hypoxic stimulation. Further treatment with histamine should then force all WPBs to fuse with the plasma membrane. Therefore, we found only a very small number of humps left on the membrane after histamine stimulation. ECs stimulated with the comparatively rather weak stimulus hypoxia still reveal more humps than histamine-treated cells. Concomitantly, the number of secretion pores increases from virtually absent in unstimulated cells up to the histamine level. Pore formation in the histamine group does not correlate with the measured vWF release. As AFM scanning starts 5 minutes after stimulation, it is left to explore whether pores have already closed or if multiple vesicle fusion occurs. Therefore, formation of exocytotic pores is a semi-quantitative indicator for vWF release.

Moreover, AFM visualized humps and pores at the apical membrane of ECs, indicating an apical release of vWF. Exocytosis of vWF by WPB fusion with the basolateral membrane can not be seen by AFM. Therefore, the number of fusion events at the basolateral membrane and the subsequent vWF release remain unclear. Apical and basolateral vWF release after WPB fusion was shown by Sporn and coworkers [39] using vWF measurements in the supernatant. However, morphological data confirming apical or basolateral secretion is missing. Using AFM, we are able to measure apical secretion of vWF. The instantaneous switch from a resting cell surface topography enriched with humps to a surface exhibiting secretion pores illustrates the membrane dynamics of endothelial cells upon hypoxic stimulation.

What could be the trigger mechanism for vWF release upon hypoxia? As reported previously, endothelial cells show a marked tolerance to hypoxia regarding their metabolism and remain well energized [23]. In this study we measured cell volume and intracellular pH of HUVEC upon hypoxic stimulation. We expected cell swelling and intracellular acidification in response to hypoxia. To our surprise, neither cell volume nor intracellular pH change during hypoxia. Moreover, our data show that endothelial cells respond adequately upon histamine stimulation even after 60 minutes of hypoxia. Therefore, it is unlikely

that metabolic alterations, such as energy deficiency, account for the acute vWF release-as already shown [23]. However, we found an elevated intracellular calcium level rising within 60 seconds upon hypoxic stimulation. As stated previously, elevated intracellular calcium levels are needed for vWF exocytosis [5, 6, 24]. The pattern of the increase of $[Ca^{2+}]_i$ depends on the stimulus and its concentration [24]. Hormones, like thrombin or histamine, induce a rapid and massive increase of $[Ca^{2+}]_i$, which is substantially more pronounced than that during hypoxia. In addition, our findings are consistent with the recent publication of Suh et al. who showed an increase of intracellular calcium in endothelial cells within 30 seconds upon chemical hypoxic stimulation induced by cyanide [40]. In that study a nonselective cation channel, namely "trp3," was suggested to be activated upon hypoxic stimulation. This channel is involved in calcium influx from the extracellular space into the cell. Park and coworkers measured a calcium influx upon hypoxic conditions by using the O_2 chelator thioglycollate in combination with a glucose-free solution [26]. In order to investigate the relevance of extracellular calcium and transmembrane calcium influx for the acute vWF exocytosis in our study, we determined the vWF release in calcium-free medium. The hypoxia-induced exocytosis is inhibited in a calcium-free medium. Moreover, an intracellular calcium release (calcium spike after histamine stimulation) was still possible, indicating unaffected intracellular Ca^{2+} stores during hypoxia. Therefore, it is likely that hypoxia activates a nonselective plasma membrane cation channel similar to previous findings, though in different cell types [40]. It has been shown that focal subplasmalemmal Ca^{2+} elevations may occur without any increase in the perinuclear region [10]. This may explain why, although we observe only a slight $[Ca^{2+}]_i$ increase in our whole-cell measurement, a high focal calcium concentration exists, localized next to the plasma membrane where Weibel Palade bodies were identified. These vesicles immediately fuse with the plasma membrane. Therefore, a small submembraneous calcium increase due to calcium influx evokes WPB fusion if WPB are close to the plasma membrane. In addition, an activation of the Na^+/Ca^{2+} exchanger under hypoxic conditions, which also leads to an increase of subplasmalemmal Ca^{2+}, was recently reported [3]. The authors suggest that the requirement for ATP leads to the activation of the Na^+-glucose cotransporter followed by the activation of the Na^+/Ca^{2+} exchanger. In contrast, histamine is followed by a distinct intracellular calcium increase and therefore recruits almost all WPB for exocytosis within 5 minutes of stimulation (3.5-fold increase of vWF release as compared to hypoxia-stimulated cells). Furthermore, calcium mobilization from intracellular stores during ischemia, due to glucose deprivation, acidosis or extracellular ATP/ADP, is likely to occur [5, 17, 42]. Schäfer and coworkers showed an intracellular calcium increase within 1 minute after application of 2-deoxy-D-glucose, an inhibitor of glycolysis. ATP contents were not affected, however, a local ATP-concentration decrease at the endoplasmic reticulum may have been possible [33]. Finally, Aono and coworkers showed that hypoxia causes both an intracellular calcium mobilization and a calcium influx [2]. Therefore, different pathophysiological stimuli that occur during ischemia may lead to an enhanced and complementary intracellular calcium increase.

The data show that the acute response of the endothelium to hypoxia happens at the plasma membrane level. Activation of a plasma membrane calcium channel followed by calcium influx or/and intracellular calcium increase and plasma membrane-associated WPB exocytosis are the early events of cell activation. An oxygen-sensing mechanism as already discussed for endothelial cells [8, 18, 28] is likely to be present in the plasma membrane, offering a seizable target for further preventive therapeutic approaches.

We thank Mrs. M. Wilhelmi for excellent work in cell culture and the gynecological staff of the Muenster Raphael and Franziskus Hospital for providing human umbilical cords.

References

1. Allen, C.B., Schneider, B.K., White, C.W. 2001. Limitations to oxygen diffusion and equilibration in in vitro cell exposure systems in hyperoxia and hypoxia. *Am. J. Physiol.* **281:**L1021–L1027
2. Aono, Y., Ariyoshi, H., Sakon, M., Ueda, A., Tsuji, Y., Kawasaki, T., Monden, M. 2000. Human umbilical vein endothelial cells (HUVECs) show Ca(2+) mobilization as well as Ca(2+) influx upon hypoxia. *J. Cell Biochem.* **78:**458–464
3. Berna, N., Arnould, T., Remacle, J., Michiels, C. 2002. Hypoxia-induced increase in intracellular calcium concentration in endothelial cells: role of the Na(+)-glucose cotransporter. *Cell Biochem.* **84:**115–131
4. Binnig, G., Quate, C.F., Gerber, C. 1986. Atomic force microscope. *Physical Reviews Letters* **56:**930–934
5. Carter, T.D., Bogle, R.G., Bjaaland, T. 1991. Spiking of intracellular calcium ion concentration in single cultured pig aortic endothelial cells stimulated with ATP or bradykinin. *Biochem. J.* **278:**697–704
6. Carter, T.D., Zupancic, G., Smith, S.M., Wheeler-Jones, C., Ogden, D. 1998. Membrane capacitance changes induced by thrombin and calcium in single endothelial cells cultured from human umbilical vein. *J. Physiol.* **513:**845–855
7. Cines, D.B., Pollak, E.S., Buck, C.A., Loscalzo, J., Zimmerman, G.A., McEver, P.P., Pober, J.S., Wick, T.M., Konkle, B.A., Schwartz, B.S., Barnathan, E.S., McCrae, K.R., Hug, B.A., Schmidt, A.M., Stern, D.M. 1998. Endothelial cells in physiology and in the pathophysiology of vascular disorders. *Blood* **91:**3527–3561
8. Faller, D.V. 1999. Endothelial cell responses to hypoxic stress. *Clin. Exp. Pharmacol. Physiol.* **26:**74–84

9. Freichel, M., Suh, S.H., Pfeifer, A., Schweig, U., Trost, C., Weissgerber, P., Biel, M., Philipp, S., Freise, D., Droogmans, G., Hofmann, F., Flockerzi, V., Nilius, B. 2001. Lack of an endothelial store-operated Ca^{2+} current impairs agonist-dependent vasorelaxation in TRP4−/− mice. *Nat. Cell Biol.* **3:**121–127
10. Graier, W.F., Paltauf-Doburzynska, J., Hill, B.J., Fleischhacker, E., Hoebel, B.C., Kostner, G.M., Sturek, M. 1998. Submaximal stimulation of porcine endothelial cells causes focal Ca^{2+} elevation beneath the cell membrane. *J. Physiol.* **506:**109–125
11. Gryczynski, I., Gryczynski, Z., Rao, G., Lakowicz, J.R. 1999. Polarization-based oxygen sensor. *Analyst* **124:**1041–1044
12. Grynkiewicz, G., Poenie, M., Tsien, R.Y. 1985. A new generation of Ca^{2+} indicators with greatly improved fluorescence properties. *J. Biol. Chem.* **260:**3440–3450
13. Haller, T., Ortmayr, J., Friedrich, F., Volkl, H., Dietl, P. 1998. Dynamics of surfactant release in alveolar type II cells. *Proc. Natl. Acad. Sci. USA.* **95:**1579–1584
14. Hamilton, K.K., Sims, P.J. 1987. Changes in cytosolic Ca^{2+} associated with von Willebrand factor release in human endothelial cells exposed to histamine. Study of microcarrier cell monolayers using the fluorescent probe indo-1. *Clin. Invest.* **79:**600–608
15. Jaffe, E.A., Nachman, R.L., Becker, C.G., Minick, C.R. 1973. Culture of human endothelial cells derived from umbilical veins. Identification by morphologic and immunologic criteria. *J. Clin. Invest.* **52:**2745–2756
16. König, J., Prenen, J., Nilius, B., Gerke, V. 1998. The annexin II-p11 complex is involved in regulated exocytosis in bovine pulmonary artery endothelial cell. *J. Biol. Chem.* **273:**19679–19684
17. Ladilov, Y., Schafer, C., Held, A., Schafer, M., Noll, T., Piper, H.M. 2000. Mechanism of Ca(2+) overload in endothelial cells exposed to simulated ischemia. *Cardiovasc. Res.* **47:**394–403
18. Lando, D., Peet, D.J., Whelan, DA, Gorman, J.J., Whitelaw, M.L. 2002. Asparagine hydroxylation of the HIF transactivation domain a hypoxic switch. *Science* **295**:858–861
19. Langer, F., Morys-Wortmann, C., Kusters, B., Storck, J. 1999. Endothelial protease-activated receptor-2 induces tissue factor expression and von Willebrand factor release. *Br. J. Haematol.* **105:**542–550
20. Le Grimellec, C., Lesniewska, E., Cachia, C., Schreiber, J.P., de Fornel, F., Goudonnet, J.P. 1994. Imaging of the membrane surface of MDCK ceils by atomic force microscopy. *Biophys. J.* 67:36–41
21. Lopes, A.A., Peranovich, T.M., Maeda, N.Y., Bydlowski, S.P. 2001. Differential effects of enzymatic treatments on the storage and secretion of von Willebrand factor by human endothelial cells. *Thromb. Res.* **101:**291–297
22. Lopez-Barneo, J., Pardal, R., Ortega-Saenz, P. 2001. Cellular mechanism of oxygen sensing. *Annu. Rev. Physiol.* **63:**259–287
23. Mertens, S., Noll, T., Spahr, R., Krutzfeldt, A., Piper, H.M. 1990. Energetic response of coronary endothelial cells to hypoxia. *Am. J. Physiol.* **258:**H689–H694
24. Nilius, B., Droogmans, G. 2001. Ion channels and their functional role in vascular endothelium. *Physiol. Rev.* **81:**1415–1459
25. Ogawa, S., Gerlach, H., Esposito, C., Pasagian-Macaulay, A., Brett, J., Stern, D. 1990. Hypoxia modulates the barrier and coagulant function of cultured bovine endothelium. Increased monolayer permeability and induction of procoagulant properties. *J. Clin. Invest.* **85:**1090–1098
26. Park, J.H., Okayama, N., Gute, D., Krsmanovic, A., Battarbee, H., Alexander, J.S. 1999. Hypoxia/aglycemia increases endothelial permeability: role of second messengers and cytoskeleton. *Am. J. Physiol.* **277:**C1066–C1074
27. Pinsky, D.J., Naka, Y., Liao, H., Oz, M.C., Wagner, D.D., Mayadas, T.N., Johnson, R.C., Hynes, R.O., Heath, M., Lawson, C.A., Stern, D.M. 1996. Hypoxia-induced exocytosis of endothelial cell Weibel-Palade bodies. A mechanism for rapid neutrophil recruitment after cardiac preservation. *J. Clin. Invest.* **97:**493–500
28. Pohl, U. 1990. Endothelial cells as part of a vascular oxygen-sensing system: hypoxia-induced release of autacoids. *Experientia* **46:**1175–1179
29. Pohlman, T.H., Harlan, J.M. 2000. Adaptive responses of the endothelium to stress. *J. Surg. Res.* **89:**85–119
30. Quist, A.P., Rhee, S.K., Lin, H., Lal, R. 2000. Physiological role of gap-junctional hemichannels. Extracellular calcium-dependent isosmotic volume regulation. *J. Cell Biol.* **148:**1063–1074
31. Rotsch, C., Jacobson, K., Radmacher, M. 1999. Dimensional and mechanical dynamics of active and stable edges in motile fibroblasts investigated by using atomic force microscopy. *Proc. Natl. Acad. Sci. U. S. A.* **96:**921–926
32. Sakariassen, K.S., Bolhuis, P.A., Sixma, J.J. 1979. Human blood platelet adhesion to artery subendothelium is mediated by factor VIII-Von Willebrand factor bound to the subendothelium. *Nature* **279:**636–638
33. Schafer, M., Bahde, D., Bosche, B., Ladilov, Y., Schafer, C., Piper, H.M., Noll, T. 2001. Modulation of early $[Ca^{2+}]_i$ rise in metabolically inhibited endothelial cells by xestospongin. *C. Am. J. Physiol.* **280:**H1002–H1010
34. Schneider, S.W. 2001. Kiss and run mechanism in exocytosis. *J. Membrane Biol.* **181:**67–76
35. Schneider, S.W., Pagel, P., Rotsch, C., Danker, T., Oberleithner, H., Radmacher, M., Schwab, A. 2000. Volume dynamics in migrating epithelial cells measured with atomic force microscopy. *Pfluegers Arch.* **439:**297–303
36. Schneider, S.W., Sritharan, K.C., Geibel, J.P., Oberleithner, H., Jena, B.P. 1997. Surface dynamics in living acinar cells imaged by atomic force microscopy: identification of plasma membrane structures involved in exocytosis. *Proc. Natl. Acad. Sci. USA.* **94:**316–321
37. Seko, Y., Enokawa, Y., Nakao, T., Yagita, H., Okumura, K., Yazaki, Y. 1996. Reduction of rat myocardial ischaemia/reperfusion injury by a synthetic selectin oligopeptide. *J. Pathol.* **178:**335–342
38. Siedlecki, C.A., Lestini, B.J., Kottke-Marchant, K.K., Eppell, S.J., Wilson, D.L., Marchant, R.E. 1996. Shear-dependent changes in the three-dimensional structure of human von Willebrand factor. *Blood* **88:**2939–2950
39. Sporn, L.A., Marder, V.J., Wagner, D.D. 1989. Differing polarity of the constitutive and regulated secretory pathways for von Willebrand factor in endothelial cells. *J. Cell Biol.* **108:**1283–1289
40. Suh, S.H., Droogmans, G., Nilius, B. 2000. Effects of cyanide and deoxyglucose on Ca^{2+} signalling in macrovascular endothelial cells. *Endothelium* **7:**155–168
41. Vischer, U.M., de Moerloose, P. 1999. von Willebrand factor: from cell biology to the clinical management of von Willebrand's disease. *Crit. Rev. Oncol. Hematol.* **30:**93–109
42. Vischer, U.M., Wollheim, C.B. 1998. Purine nucleotides induce regulated secretion of von Willebrand factor: involvement of cytosolic Ca^{2+} and cyclic adenosine monophosphate-dependent signaling in endothelial exocytosis. *Blood* **91**:118–127
43. Wagner, D.D. 1990. Cell biology of von Willebrand factor. *Annu. Rev. Cell Biol.* **6:**217–246